

Stretchable phosphorescent polymers by multiphase engineering

Received: 3 November 2023

Accepted: 9 April 2024

Published online: 15 May 2024

Nan Gan¹, Xin Zou¹, Zhao Qian², Anqi Lv³, Lan Wang³, Huili Ma³, Hu-Jun Qian², Long Gu^{1,4}✉, Zhongfu An³✉ & Wei Huang^{1,3}✉

Stretchable phosphorescence materials potentially enable applications in diverse advanced fields in wearable electronics. However, achieving room-temperature phosphorescence materials simultaneously featuring long-lived emission and good stretchability is challenging because it is hard to balance the rigidity and flexibility in the same polymer. Here we present a multiphase engineering for obtaining stretchable phosphorescent materials by combining stiffness and softness simultaneously in well-designed block copolymers. Due to the microphase separation, copolymers demonstrate an intrinsic stretchability of 712%, maintaining an ultralong phosphorescence lifetime of up to 981.11 ms. This multiphase engineering is generally applicable to a series of binary and ternary initiator systems with color-tunable phosphorescence in the visible range. Moreover, these copolymers enable multi-level volumetric data encryption and stretchable afterglow display. This work provides a fundamental understanding of the nanostructures and material properties for designing stretchable materials and extends the potential of phosphorescence polymers.

Stretchable and flexible materials are highly desirable for developing flexible electronics^{1–4}. Wherein stretchable luminescent materials as vital components can provide emission sources and intrinsic flexibility to the optoelectronic displays for versatile applications in soft robots, intelligent sensing/detection, on-skin displays, and wireless communication (Fig. 1a)^{5–9}. To date, most of the reported stretchable emitters are based on fluorescent polymers that only harness singlet excitons and suffer from short lifetimes^{10–12}. Rare stretchable phosphorescent materials for advanced applications have been developed. Room-temperature phosphorescence (RTP) materials, featuring long emission lifetimes, tunable excited state properties, and high exciton utilization, have recently received increasing attention^{13–16}. To obtain organic RTP materials, tremendous efforts have been devoted to promoting the intersystem crossing (ISC) process by incorporating heavy atoms, heteroatoms, and aromatic carbonyls into phosphors^{17–20}, and restraining

the non-radiative decay of triplet excitons by building a rigid environment^{21,22}. Given the intrinsic merits of polymers in good processability, lightweight, and flexibility, polymer-based RTP materials become attractive alternatives to small molecules for expanding applications in stretchable photoelectronics^{23–25}. Conventionally, RTP polymers can be obtained by chemically conjugating phosphors onto a polymer backbone via polymerization^{26–28}, or doping chromophores into rigid polymer hosts^{29–32}. These homopolymers with rich hydrogen bonds and rigid microenvironments could suppress the non-radiative decay of phosphors for efficient RTP. However, the small free volume and high glass transition temperature (T_g) limit the movement and rearrangement of polymer chains, resulting in poor mechanical deformations. Generally, stretchable polymers require a low T_g to meet the fast segmental dynamics at room temperature, which will cause intensive non-radiative deactivation and weaken RTP performance.

¹Frontiers Science Center for Flexible Electronics (FSCFE), MIIT Key Laboratory of Flexible Electronics (KLoFE), Northwestern Polytechnical University, Xi'an 710072, China. ²State Key Laboratory of Supramolecular Structure and Materials, Institute of Theoretical Chemistry, College of Chemistry, Jilin University, Changchun 130012, China. ³Key Laboratory of Flexible Electronics (KLoFE) & Institute of Advanced Materials (IAM), Nanjing Tech University (NanjingTech), 30 South Puzhu Road, Nanjing 211816, China. ⁴Research and Development Institute of Northwestern Polytechnical University in Shenzhen, Shenzhen 518057, China. ✉ e-mail: iamlgu@nwpu.edu.cn; iamzfan@njtech.edu.cn; vc@nwpu.edu.cn

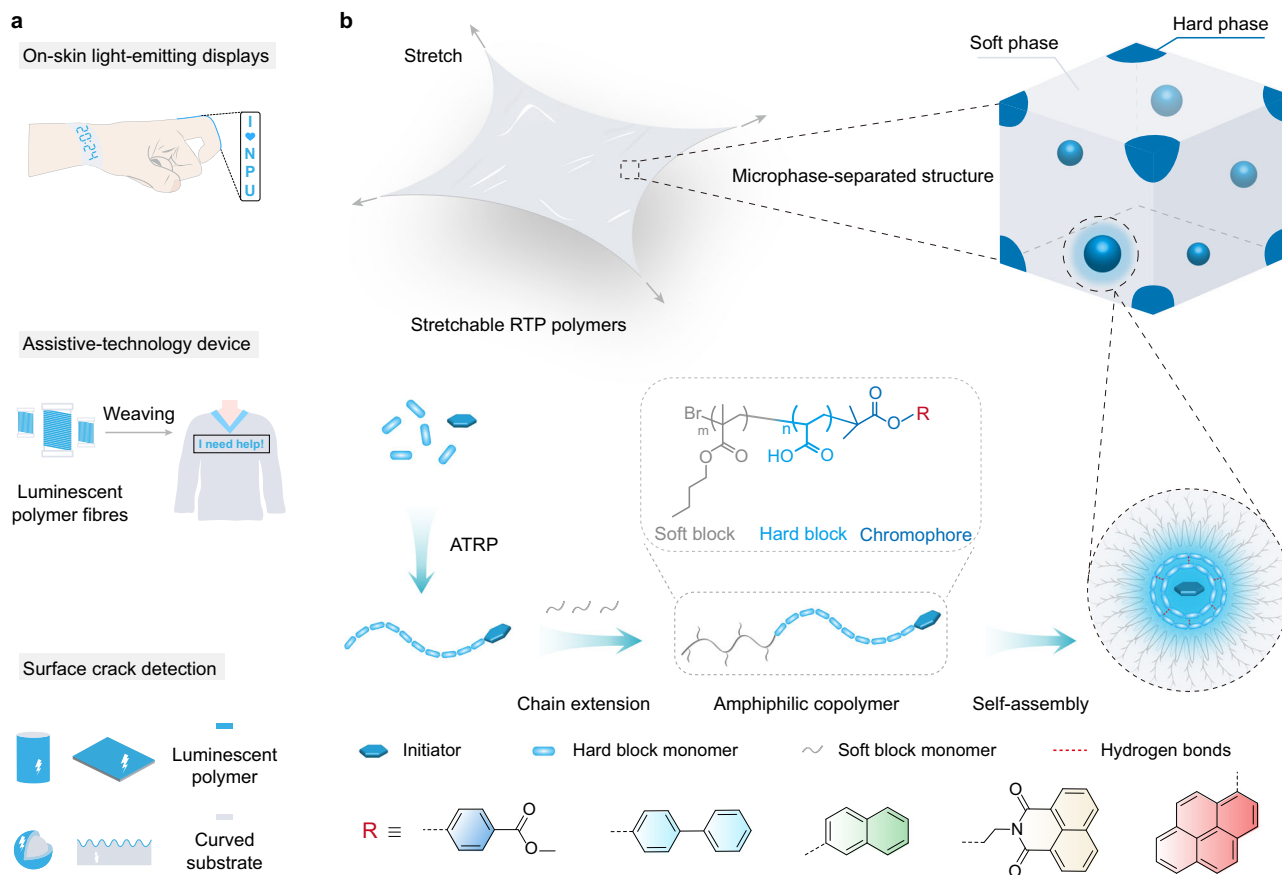


Fig. 1 | Potential applications and design concept of stretchable phosphorescent materials. **a** Potential application scenarios of stretchable luminescent materials in displays, sensing, and detection. **b** Rational design of stretchable room-temperature phosphorescence (RTP) polymers. Utilizing a two-step atom-transfer radical polymerization (ATRP) and subsequent hydrolysis, amphiphilic polyacrylic acid-co-poly (alkyl methacrylate) block copolymers are achieved. During

hydrolysis, the block copolymer self-assembles into two-phase nanostructures. The polyacrylic acid hard phase with rich hydrogen bonding protects the phosphors for RTP generation, and the poly (butyl methacrylate) soft phase contributes to dissipating strain energy and thus enhancing stretchability. Meanwhile, stretchable copolymers with color-tunable RTP can be developed by rationally tailoring the initiator components and energy levels.

Therefore, achieving intrinsically stretchable polymers with long-lived phosphorescence remains a challenge.

Multiphase engineering could provide a facile platform to combine different components with multi-functions into a block copolymer^{33–35}. Generally, block copolymers consist of two or more thermodynamic incompatible polymer segments linked by the covalent bond. The immiscibility of dissimilar segments generally induces a self-assembly process and forms periodic microphase-separated nanostructures^{36–39}. These multiple microdomains can transfer or amplify their functions to the macroscopic scale of materials, thus giving rise to a portfolio of distinctly different properties in the same copolymer. Inspired by this, we reason that stretchable RTP materials might be obtained by multiphase engineering. This approach can efficiently combine stiffness and softness in the same polymer via programming the rigid microphase in the continuous soft domain of a block copolymer.

Here, we adopt atom-transfer radical polymerization (ATRP) to prepare block copolymers because of the precisely controlled molecular weight, composition, on-demand functionality, and wide utilization for diverse monomers⁴⁰. A naphthalimide derivative is selected as ATRP initiator and phosphorescence chromophore because the multiple carbonyl groups and nitrogen heteroatom could effectively facilitate the population of triplet states through an efficient ISC process. Moreover, the rigid planar molecular skeletons can restrict molecular motions for suppressed non-radiative decay, contributing to RTP generation^{41,42}. Considering the rich carboxyl groups can form

strong hydrogen bonds to suppress the non-radiative transition of triplet excitons, we choose polyacrylic acid (PAA) as the hard block²⁴. Meanwhile, soft monomeric units, including alkyl (meth)acrylates, carbosilane, siloxane, and ether chain, are widely used to decrease the T_g for improving the flexibility or stretchability of polymer^{43–45}. Particularly, alkyl methacrylate shows high ATRP activity, and the hydrophobic alkyl chains favor preventing phosphors from being quenched by surrounding moisture. Therefore, alkyl methacrylate monomers are introduced to prepare the soft blocks (Fig. 1b). After self-assembly of amphiphilic block copolymers, hard-soft microphase-separated structures can be formed. Wherein dispersed PAA hard phase provides a rigid environment to protect triplet excitons and thus promote the RTP generation. Continuous poly (alkyl methacrylate) phase with soft alkyl chains can enhance polymer chain dynamics, guaranteeing the stretchability of copolymers. Meanwhile, their mechanical performance can be well-tuned by varying the molecular structure and content of the soft blocks. Benefitting from multiphase engineering, stretchable RTP materials can be obtained.

Results

Materials synthesis and characterizations

Multiphase block copolymers were prepared by a two-step ATRP and subsequent hydrolysis process (Supplementary Figs. 1–5). We synthesized bromoisobutyrate-modified naphthalimide (DBI) as the ATRP initiator. Then, macroinitiator PBM was synthesized with DBI, *tert*-butyl acrylate, $\text{CuBr}_2/\text{TPMA}$ (catalyst), and $\text{Cu}(0)$ mixtures under nitrogen at

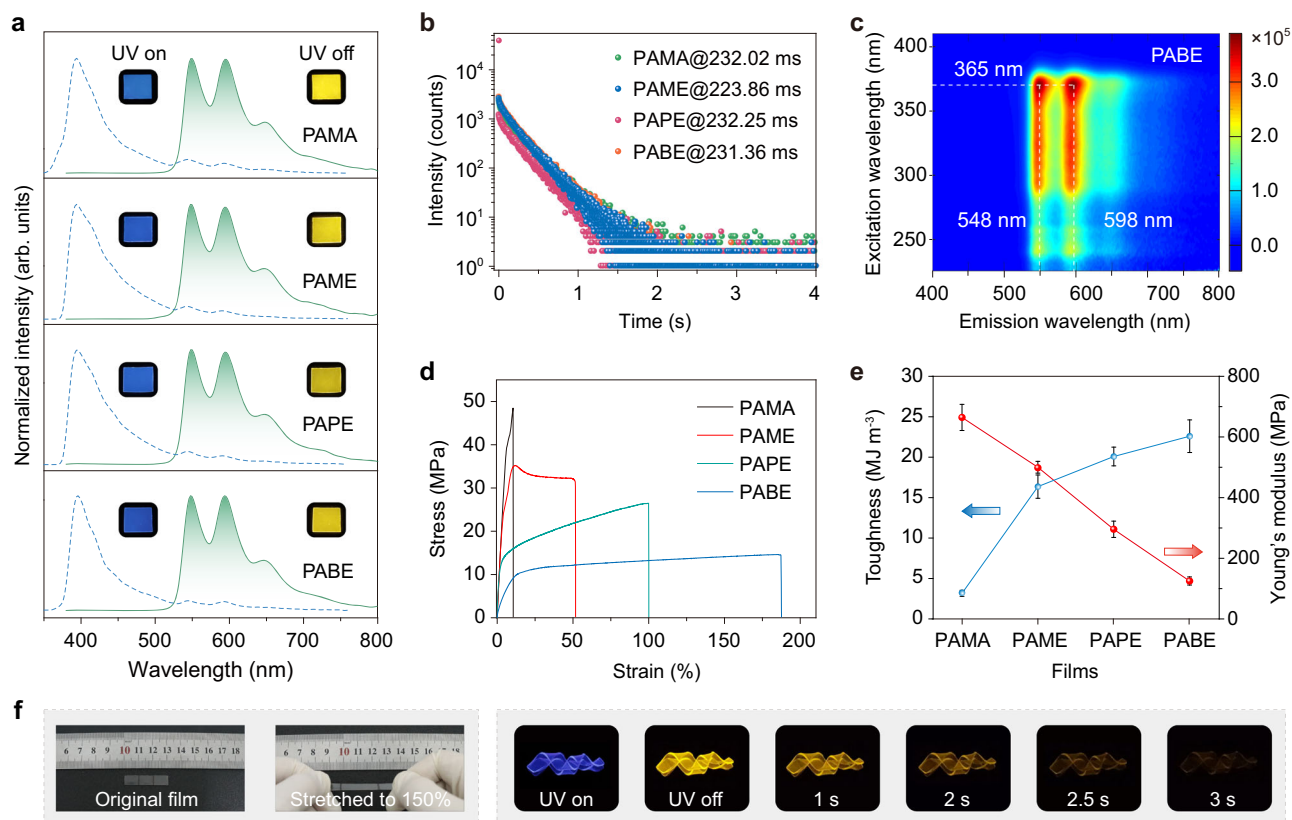


Fig. 2 | Photophysical and mechanical properties of PAMA, PAME, PAPE, and PABE block copolymers. **a** Normalized steady-state photoluminescence (blue lines) and phosphorescence (green lines) spectra of copolymers PAMA to PABE. Insets show corresponding photographs under 365 nm UV lamp on and off. **b** Lifetime decay curves of emission bands at 548 nm. **c** Excitation-phosphorescence mapping of PABE film under ambient conditions. **d** Typical

stress-strain curves of polymer PAMA to PABE films, indicating tunability of the mechanical properties through rational molecular design. **e** Toughness and Young's modulus variation of PAMA to PABE films. Error bars represent mean \pm standard deviation ($n = 3$). **f** Deformability and ultralong RTP demonstration of PABE film.

room temperature, followed by next chain extension utilizing PBM, alkyl methacrylate monomer, $\text{CuCl}_2/\text{PMDETA}$ (catalyst), and stannous octoate in a given ratio. After the reaction finished, the mixture was precipitated in methanol/ H_2O to give the as-prepared block copolymer, which was further dissolved in dichloromethane/trifluoroacetic acid mixture and hydrolyzed at room temperature for 24 h to give the final amphiphilic block copolymer. Considering the alkyl side chain lengths will influence T_g and thus chain dynamics of corresponding copolymers, we selected methyl methacrylate (MMA), ethyl methacrylate (EMA), propyl methacrylate (PMA), and butyl methacrylate (BMA) as the second block monomers for preparing amphiphilic block copolymers PAMA, PAME, PAPE, and PABE, respectively. The chemical structures and purity of ATRP initiators were fully confirmed by nuclear magnetic resonance (^1H and ^{13}C NMR) spectroscopy, high-performance liquid chromatography-mass spectrometry (HPLC-MS), and elemental analyses (Supplementary Figs. 6–34). As demonstrated by Fourier transform infrared spectroscopy (FTIR) spectra, the hydroxy stretch at around $3100\text{--}3600\text{ cm}^{-1}$ indicated that the *tert*-butyl ester groups were converted into carboxyl moieties after hydrolyzation, and the shift of carbonyl stretching resonance verified the formation of the $\text{C}=\text{O}\cdots\text{H}-\text{O}$ hydrogen bonds (Supplementary Fig. 35). The resulting polymer molecular weight and polydispersity (PD) were determined by gel permeation chromatography (GPC) (Supplementary Figs. 36–39 and Supplementary Tables 1–3).

Photophysical and mechanical studies

To understand the influence of alkyl side chain lengths of the soft block on the copolymer performance, we investigated the photophysical

properties of PAMA, PAME, PAPE, and PABE containing equimolar acrylic acid (AA) and soft block monomers. Under 365 nm excitation, all films displayed blue emission colors with photoluminescence (PL) bands at 395 nm (Fig. 2a and Supplementary Fig. 40). After stopping the ultraviolet (UV) lamp excitation, intense yellow afterglow lasting for 3 s can be observed (Supplementary Fig. 41 and Supplementary Movie 1). With a delay time of 8 ms, PAMA to PABE showed identical spectra with prominent peaks at 548 and 598 nm. Meanwhile, their lifetime decay profiles at 548 nm exhibited almost equal lifetimes up to 232.25 ms, indicating the phosphorescence characteristic (Fig. 2b and Supplementary Table 4). Additionally, phosphorescence spectra remain constant emission bands under varied excitation wavelengths, suggesting stable triplet emissive centers deriving from DBI units in these multiphase systems (Fig. 2c and Supplementary Fig. 42). These results are consistent with control polymers HPAA and NPAA, indicating the incorporation of soft segments with different species from MMA to BMA as well as the terminal bromine atom at the polymer chain had little impact on the photophysical properties of these block copolymers, but significantly affected their mechanical properties (Supplementary Figs. 43, 44 and Supplementary Tables 5, 6). As shown in Fig. 2d and e, compared with homopolymer HPAA, the strain-at-break of block copolymers had a dramatic enhancement and increased gradually as increasing alkyl side chain length of the soft blocks, with a maximum of 188% for PABE film (Supplementary Fig. 45). The calculated toughness, related to energy dissipation, showed the highest value of 23.6 MJ m^{-3} in PABE film (Supplementary Fig. 46 and Supplementary Table 7). In contrast, fracture strength and Young's modulus decreased from PAMA to PABE films, consistent with the varying trend

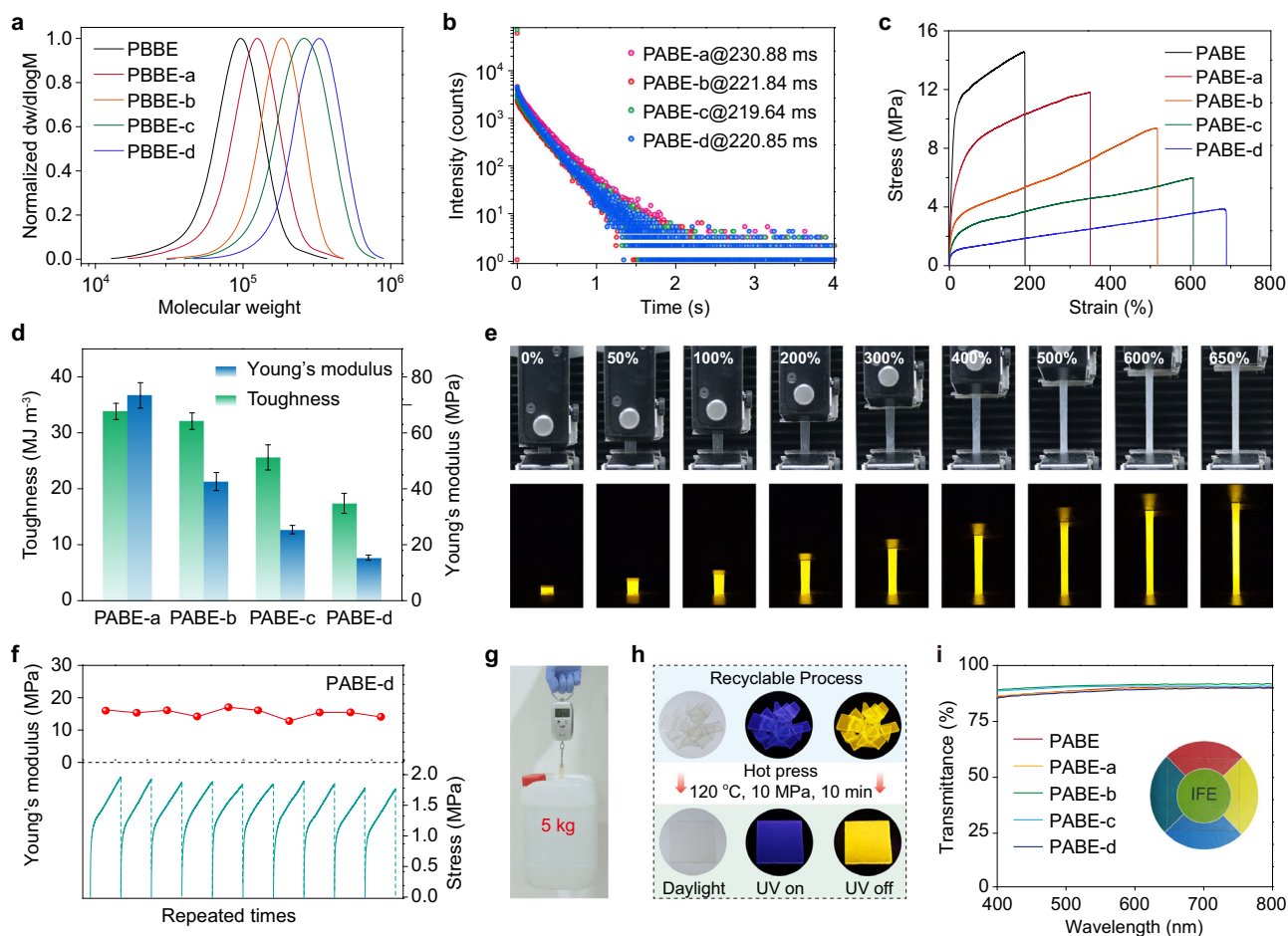


Fig. 3 | Photophysical and mechanical properties of PABEs with varying BMA mass fraction. **a** GPC traces of the unhydrolyzed copolymers PBBE to PBBE-d. The molecular weight (M_n) can further determine the content of AA and BMA in PABE to PABE-d. According to the living character of ATRP, the molar ratio of AA/BMA was 1:1, 1:3, 1:5, 1:7, and 1:9, respectively. **b** Lifetime decay curves of emission bands at 548 nm. **c** Stress-strain curves of PABE to PABE-d films. **d** Calculated toughness and Young's modulus of copolymers PABE-a to PABE-d. Error bars represent mean \pm standard deviation ($n = 3$). **e** Real-time photographs of PABE-d film during stretching on a universal testing machine taken under daylight and after stopping

the 365 nm excitation. **f** Repeated tensile tests of PABE-d film with a 200% strain 20 times (each repeated test needs some recovery times for the sample). The green lines show the stress-strain curves at the 2nd, 4th, 6th to 20th tests, and the red balls represent related Young's modulus. **g** Photograph of PABE-d film when lifted with heavy loads. **h** Photographs of the cut PABE-d film pieces and after hot pressing (120 °C, 10 MPa, 10 min), demonstrating its good recyclability. **i** Optical transmittance of various PABEs films in the visible range. Inset: photograph of PABE film (thickness: 0.4 mm).

of their T_g , demonstrating lower stiffness and easier deformation for PABE film (Supplementary Figs. 47–49). Therefore, stretchable and flexible RTP polymer can be achieved by synthesizing amphiphilic block copolymers (Fig. 2f). Moreover, increasing alkyl side chain lengths of the soft blocks can effectively enhance polymer chain dynamics and improve stretchability.

To further optimize the mechanical properties of the copolymer, we synthesized PABE-a to PABE-d with varied molecular weights of the soft blocks (Fig. 3a and Supplementary Table 2). As shown in Fig. 3b, as the molecular weight increased gradually, the photophysical properties of PABE-a to PABE-d films were almost unchanged, maintaining long-lived phosphorescence lifetimes over 220 ms (Supplementary Figs. 50–52 and Supplementary Tables 8, 9). In contrast, the mechanical performance obviously depended on the BMA content. As the molar ratio of AA/BMA changed from 1/3 to 1/9, the stretchability of the copolymer films significantly improved from 350% to 690%, far exceeding the reported homogeneous RTP polymer films, and PABE-d film could keep an elongation of beyond 600% when the tensile rate was below 50 mm min⁻¹ (Fig. 3c, Supplementary Figs. 53, 54, and Supplementary Table 10). Meanwhile, as relative proportion of acrylic acid decreased, the toughness of PABE to PABE-d films decreased from 33.8

to 17.4 MJ m⁻³, and Young's modulus reduced from 112.8 to 15.4 MPa (Fig. 3d and Supplementary Table 11). From these experiments, we found that varying molecule weights of the PBMA block can significantly regulate the mechanical properties of copolymers but almost not affect the ultralong phosphorescence. In agreement with our multiphase design concept, the PAA hard block not only provides the rigid microenvironment for generating RTP but also serves as the physical cross-linking point to modulate the stiffness of copolymers. While the PBMA soft block mainly determines the elongation ability of PABEs samples.

Given the decent performance of PABE-d film, we next investigated the optical and mechanical stabilities. As shown in Fig. 3e, PABE-d film can maintain bright ultralong RTP under different stress and strain conditions (Supplementary Figs. 55, 56 and Supplementary Movie 2). Moreover, it can be repeatedly stretched to a 200% strain 20 times with stable Young's modulus, after which it can still hold a weight of 5 kg (Fig. 3f and g). These results suggested their good mechanical durability and optical stability under large-strain states. Furthermore, benefiting from the high thermal stability and softness of the PBMA segment, PABE-d film performed good recyclability via hot pressing (Fig. 3h and Supplementary Figs. 57, 58). Therefore, our ingenious

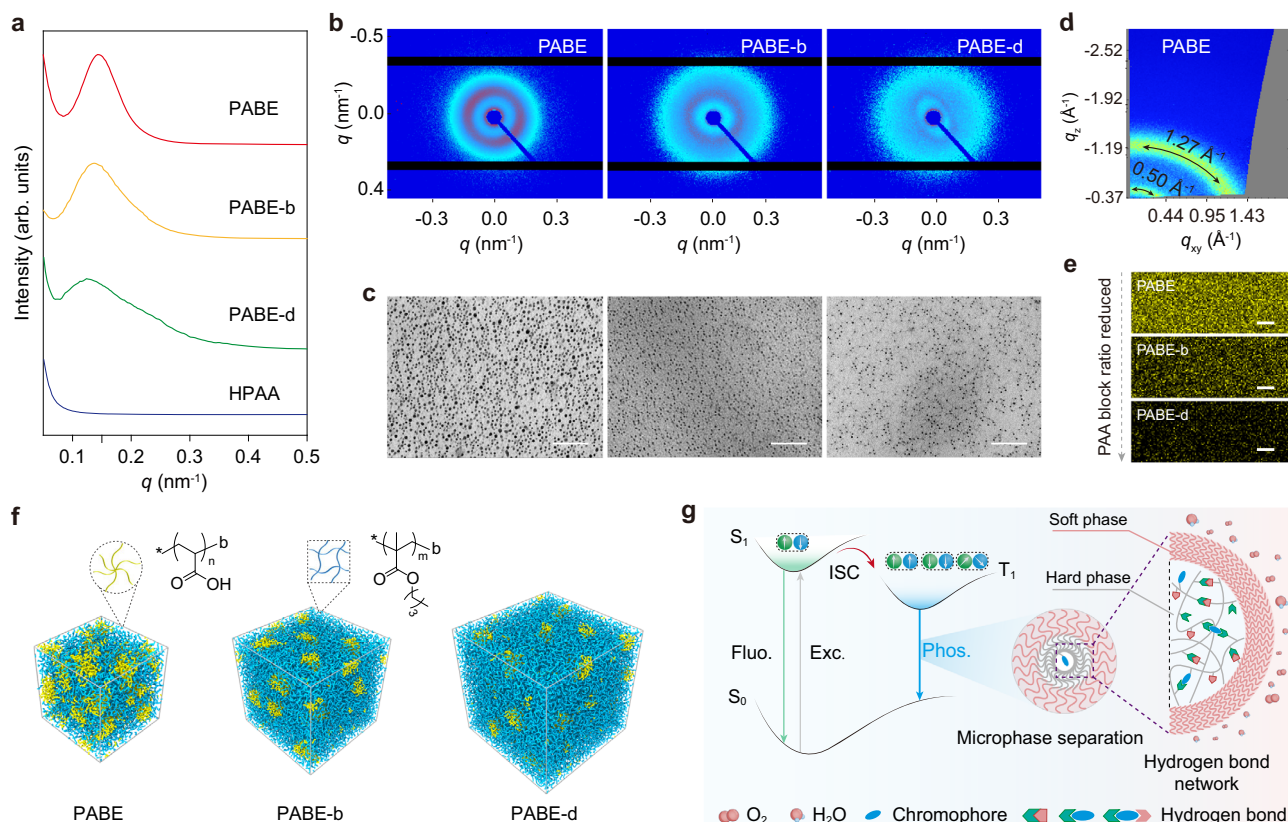


Fig. 4 | Mechanism of stretchable polymers with ultralong phosphorescence.

a SAXS profile plots of copolymers PABEs and homopolymer HPAA, supporting the microphase-separated morphology in the designed block copolymers, while HPAA shows no scattering peak. **b** Related 2D SAXS images of PABEs films. **c** TEM images of PABE (left), PABE-b (middle), and PABE-d (right) provide clear evidence of the microphase-separated structure with PAA phase (dark spheres with diameters of 10–30 nm) dispersed in continuous PBMA phase (gray areas). The PAA segment was selectively stained with uranyl acetate. Scale bar: 300 nm. **d** 2D-WAXS pattern of

PABE film. **e** Confocal fluorescence images of PABE, PABE-b, and PABE-d. $\lambda_{\text{ex}} = 405$ nm. Scale bar: 20 μm . Yellow channel (570–600 nm): phosphorescence of DBI in PAA matrix. **f** Snapshots of the simulated structures for PABE, PABE-b, and PABE-d in the bulk. These amphiphilic copolymers spontaneously assemble into microphase-separated structures. **g** Proposed mechanism of ultralong phosphorescence from amphiphilic block copolymers. Fluo., Phos., and Exc. refer to fluorescence, phosphorescence, and excitation, respectively.

multiphase design endows block copolymers with integrated advantages in good mechanical properties, optical and thermal stability, recyclability, water resistance, and ultralong phosphorescence, providing a facile strategy for obtaining stretchable RTP materials (Supplementary Figs. 59, 60). Additionally, despite our designed copolymers consisting of immiscible PAA and PBMA segments, they exhibit high optical transparency of up to 90% in the visible region, indicating good uniformity and no macroscopic phase separation of these polymers (Fig. 3i). Based on these data, we speculate that there might form microphase-separated structures in these block copolymers contributing to their decent stretchability and RTP performance.

Mechanism of stretchable phosphorescent copolymers

To confirm our speculation, we further systematically investigated the microstructures of various PABEs films. As shown in Fig. 4a, small-angle X-ray scattering (SAXS) profile plots displayed broad and intense scattering peaks for PABE, PABE-b, and PABE-d films, whereas no obvious scattering peaks can be detected from polymers PBBE and HPAA (Supplementary Fig. 61). This result indicated the formation of multiple microphases in PABEs copolymer films. Moreover, from PABE to PABE-d, the scattering peaks gradually shifted to the low q region along with decreased intensity, indicating increased inter-domain spacings ($d = 2\pi/q$) and less prominent accumulation of the hard segments, thus reducing Young's modulus. The 2D SAXS images showed that electron density contrast between the two domains decreased as PAA contents reduced, proving that the immiscibility of soft-hard

blocks, as well as hydrogen bonds between PAA chains, could provide the driving force for microphase separation (Fig. 4b)^{46,47}. The microphase-separated nanostructures were further certified by transmission electron microscopy (TEM) utilizing ultra-thin section specimen (Fig. 4c). The TEM micrographs reveal clear two-phase morphology, wherein spherical PAA hard phases were uniformly dispersed in continuous PBMA soft phase. As the ratio of AA/BMA varied from 1/1 to 1/9, the soft domains increased with larger inter-domain spacings, in accordance with the SAXS results. This variation presumably contributes to the different stretchability of PABEs films. Additionally, all PABEs films showed T_g at around 25 °C, providing a prerequisite for chain segmental motion to achieve flexibility and stretchability of copolymers at room temperature. Importantly, this low T_g was consistent with that of homopolymer PBMA, indicating the stretchability of resulting copolymers mainly derived from the soft PBMA block (Supplementary Fig. 62). These data agree with the multiphase design concept, wherein the soft microphase provides fast segmental dynamics for good stretchability of copolymers.

To further reveal the origination of ultralong RTP, we conduct wide-angle X-ray scattering (WAXS) experiments of various copolymers. As shown in Fig. 4d, only two broad scattering bands at 0.50 \AA^{-1} (7.11°) and 1.27 \AA^{-1} (18.00°) ascribed to the characteristic bands from PBMA can be observed, without other aggregates-induced π - π interactions (Supplementary Figs. 63–67). Combining the photophysical properties of DBI in doped-PAA film and dilute solution (10^{-5} M) at 77 K, we infer that ultralong RTP at 548 nm of PABEs copolymers derived

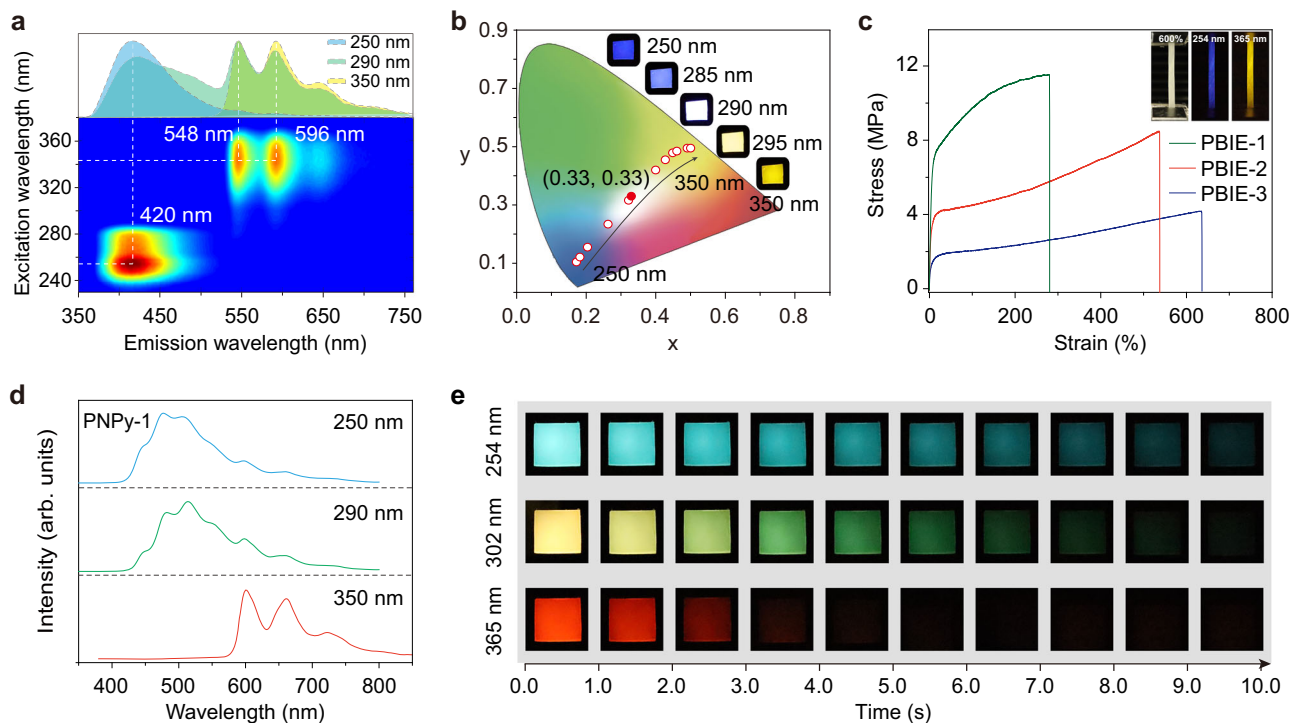


Fig. 5 | Stretchable polymers with color-tunable ultralong phosphorescence. **a** Excitation-phosphorescence mapping and phosphorescence spectra of PBIE-1 film excited by 250, 290, and 350 nm. **b** CIE chromaticity diagram for copolymer PBIE-1 with excitation ranging from 250 to 350 nm. Inset: long-lived phosphorescence photographs of PBIE-1 excited at 250, 285, 290, 295 and 350 nm, respectively.

c Stress-strain curves of PBIE-1 to PBIE-3 films. Inset: photographs of PBIE-3 film with a 600% strain taken under daylight and after stopping the 254 and 365 nm excitation. **d** Phosphorescence spectra of PNPY-1 film excited by 250, 290, and 350 nm. **e** Excitation- and time-dependent phosphorescence photographs of PNPY-1 taken after ceasing the 254, 302, and 365 nm irradiation.

from the isolate molecule phosphorescence of DBI chromophore in the hard PAA phase (Supplementary Figs. 68–73). Meanwhile, we utilized confocal fluorescence microscopy to trace the RTP origination in our multiphase systems (Fig. 4e). Under 405 nm laser irradiation, the collected yellow channel imaging demonstrated that the emitting centers were uniformly dispersed in films. As the content of the hard block decreased, the emission areas became sparse, which accorded with the variation tendency of the PAA microphase distribution in the TEM images. This result indicates that the ultralong phosphorescence of these copolymers mainly originated from the hard PAA microphase, which can confine phosphors via multiple hydrogen bonds. Additional control experiments can also verify this description. Due to the lack of strong hydrogen bonds, almost no RTP was observed from control polymers PBM, PBBE-a, and PBMA under ambient conditions (Supplementary Figs. 74–77). Therefore, we conclude that the hard and soft phases based on multiphase engineering are indispensable for achieving stretchable RTP polymers.

To strengthen our conclusions, large-scale coarse-grained molecular dynamics simulations were performed to reveal the self-assembly behavior and multiple microphase formation of these block copolymers (Supplementary Tables 12, 13, Supplementary Data 1). As shown in Fig. 4f, after $1.2 \times 10^6 \tau$ simulation, microphase-separated structures of amphiphilic block copolymers PABE, PABE-b, and PABE-d in the bulk are obtained. With increasing the volume fractions of the soft block, the PAA microphase was widely distributed in the PBMA domain with larger inter-domain spacings (Supplementary Fig. 78). These theoretical simulation results agree well with the SAXS and TEM data, illustrating the formation of hard-soft microphase-separated structures in these block copolymers.

Taken together, we proposed a reasonable mechanism for stretchable RTP copolymers. As shown in Fig. 4g, benefitting from the multiphase design, amphiphilic block copolymers self-assemble into microphase-separated structures, wherein dispersed hard phases are

uniformly embedded in the continuous soft phase. The hard microphase contains chromophores and PAA chains. Under the UV lamp excitation, triplet excitons can be populated through the ISC process (Supplementary Fig. 79, Supplementary Data 2). Due to the multiple hydrogen bonds between polymer chains and chromophores, the hard phase provides a rigid microenvironment to confine molecular motions of chromophores and decrease the quenching from surrounding oxygen. Therefore, the triplet state excitons are stabilized and non-radiative transition is effectively suppressed for generating ultralong RTP (Supplementary Fig. 75). Meanwhile, the PBMA soft phase with a low T_g plays a crucial role in enhancing the polymer chain dynamics, thereby rendering a decent stretchability for the block copolymers (Supplementary Fig. 80). Besides, the tangled hydrophobic soft segments provide an extra barrier for the triplet excitons and further prevent the quenching from surrounding moisture. Under the synergism of hard and soft microdomains, copolymers featuring ultralong RTP, decent mechanical properties, thermal and optical stability, and water resistance can be achieved.

The universality of the multiphase engineering

To establish the generality of multiphase engineering, stretchable copolymers with color-tunable RTP were further developed by rationally tailoring the initiator components and energy levels (Supplementary Fig. 79). We expand the binary initiator system PBIEs (Supplementary Figs. 81–84). As excitation wavelengths varied from 230 to 380 nm, the RTP emission center showed a dramatic bathochromic shift from 420 to 548 nm (Fig. 5a and Supplementary Table 14). Notably, under 290 nm excitation, pure white phosphorescence with CIE coordinate of (0.33, 0.33) can be achieved, along with tunable mechanical properties (Fig. 5b, c, and Supplementary Table 15). Meanwhile, the ternary initiator system PNPys can further expand the RTP color tunability ranging from 476 to 600 nm with ultralong lifetimes of 981.11, 863.02, and 244.06 ms, respectively

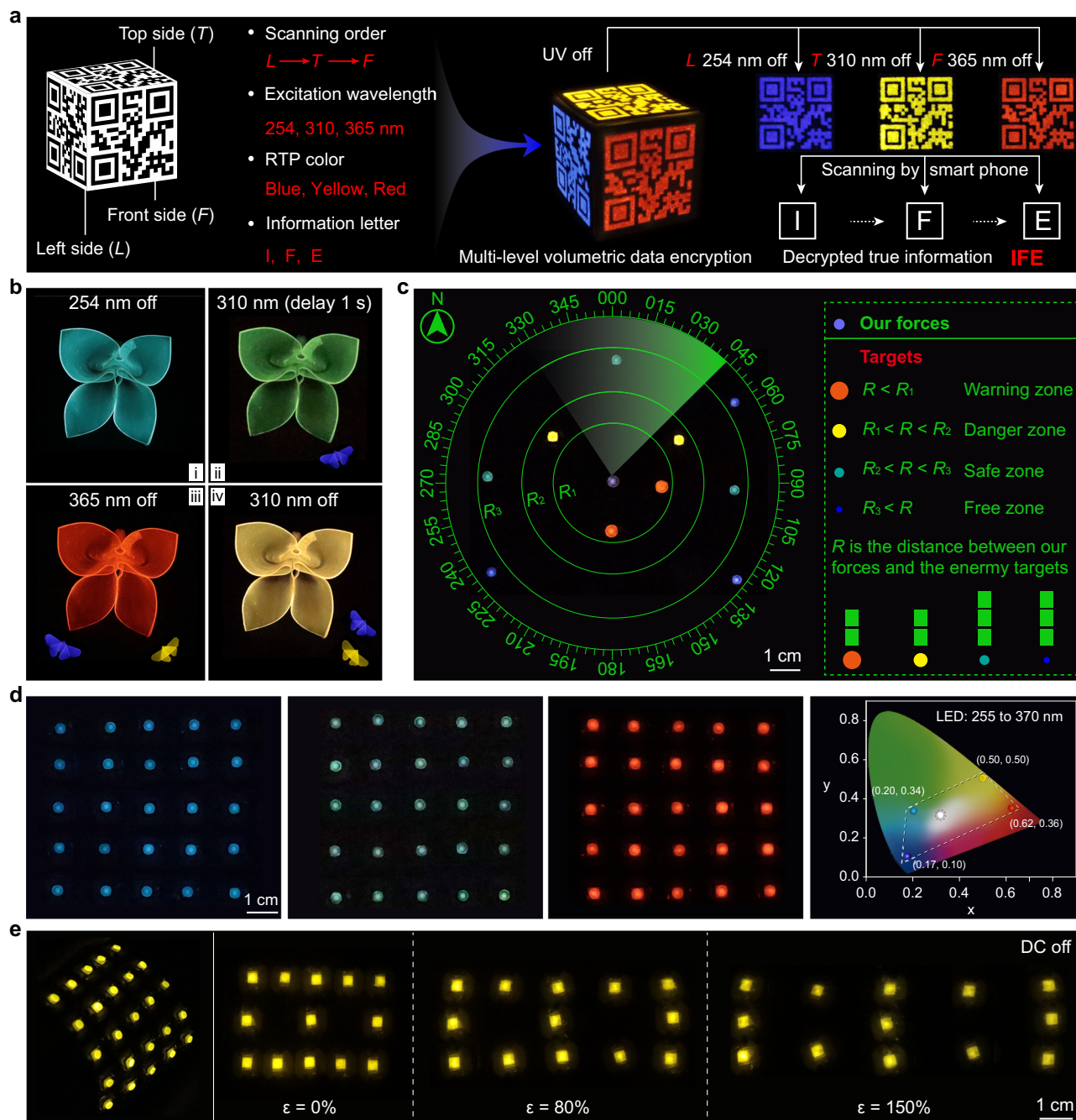


Fig. 6 | Demonstration of stretchable phosphorescent polymers for multi-level data encryption and multicolor afterglow display. **a** Schematic illustration of multi-level volumetric data encryption utilizing PBIE-3 (L and T sides) and PNPY-3 (F side) samples, and photographs of the QR codes on a cube after switching off different UV lamps and the corresponding screenshot of the identified letters I, F, and E. **b** Photographs of the hand-folded flower (PNPy-3 film) and butterfly (PBIE-3 film) taken after stopping different UV light excitations. **c** Demonstration of radar

detection mimicry by controlling direct current (DC) off. **d** RGB afterglow display arrays based on PNPY-3 films under DC switched off. The CIE chromaticity diagram shows the wide gamut coverage of PNPY-3 and PBIE-3 films under different LED light excitations, demonstrating the potential of color-tunable copolymers in full-color displays. **e** Demonstration of the display arrays subjected to bending and stretching to different strains under DC switched off.

(Fig. 5d, e, Supplementary Figs. 85–89, and Supplementary Tables 16, 17). Notably, PNPY-3 film displayed a maximum elongation of up to 712%. Besides, stretchable copolymer films with efficient RTP can also be obtained by utilizing Br-modified phosphors (Supplementary Figs. 90, 91 and Supplementary Table 18).

Potential applications

Combining the color-tunable RTP and stretchability of these block copolymers, we explored their potential in data encryption and

flexible multicolor afterglow display. As shown in Fig. 6a, based on screen printing, three quick response (QR) codes carrying I, F, and E information were painted on different sides of a cube. Only when we obey the right excitation wavelength, RTP color, and scanning order can we get the true information IFE, demonstrating the potential of our block copolymers in multi-level volumetric information encryption (Supplementary Fig. 92, Supplementary Movie 3). Meanwhile, the flexible copolymer films can be made into different handicrafts for information storage. Due to the dynamic afterglow of PNPY-3 and

PBIE-3 films, the variation of a flower from budding in spring to withering in autumn, accompanied by the butterflies attracted and then flying away was recorded, which can be potentially applied in instant information recording and reading (Fig. 6b, Supplementary Fig. 93). Besides, a multicolor afterglow display can be realized in one copolymer film by controlling electrical excitation (Supplementary Figs. 94–103, Supplementary Table 19). Color-tunable RTP copolymer films were utilized as display screens and circuit diagram was introduced to fabricate the photoelectric device for afterglow display. As shown in Fig. 6c, a demo of radar all-round detection can be realized by controlling direct current (DC) off (Supplementary Movie 4). The colorful afterglow represents the targets in different ranges, demonstrating the potential of these copolymers for accurate positioning and warning. Furthermore, the stretchable copolymer films can also be utilized for large-area full-color afterglow display (5×5 -pixel array), while maintaining their resistance to large mechanical deformation, including bending and stretching up to 150% strain (Fig. 6d, e, and Supplementary Movie 5).

Discussion

In conclusion, we have presented a multiphase design strategy for stretchable phosphorescent materials that combine stiffness and softness into an amphiphilic block copolymer. The well-defined design and ATRP synthesis offer versatility in tuning polymer structures and mechanical properties. Impressively, the maximum tensile strain could reach up to 712%, maintaining an ultralong phosphorescence lifetime of 981 ms. The ultralong RTP could be observed even under repeated strain, demonstrating good mechanical durability and optical stability. The long-lived RTP was ascribed to the formation of microphase-separated nanostructures in copolymers. Besides, multiphase engineering could generally apply to the binary and ternary initiator systems for realizing color-tunable phosphorescence in the visible range. We also demonstrated their potential in multi-level volumetric data encryption and stretchable multicolor afterglow display combining stretchability and color-tunable phosphorescence. This work will provide a platform for designing intrinsically stretchable phosphorescent materials and extend the potential of phosphorescence polymers.

Methods

Reagents and materials

tert-Butyl acrylate (TBA, 99%), cupric bromide (CuBr_2 , 99.9%), tris(2-pyridylmethyl)amine (TPMA, 98%), *N,N*-dimethylformamide (DMF, 99.8%), methanol (MeOH, 99.9%), butyl methacrylate (BMA, 99%), cupric chloride (CuCl_2 , 98%), pentamethyldiethylenetriamine (PMDETA, 98%), anisole (99%), stannous octoate (95%), tetrahydrofuran (THF, 99.5%), dichloromethane (DCM, 99.5%), trifluoroacetic acid (TFA, 99.5%), methylparaben (99%), triethylamine (99.5%), 2-bromoisobutyl bromide (98%), 4-phenylphenol (99%), 2-naphthol (99%), 1,8-naphthalic anhydride (99%), ethanolamine (99%), ethanol (99.9%), and 1-hydroxypyrene (98%) were purchased from commercial sources without further purification unless otherwise stated. All the purchased monomers were purified by passing through a column of basic alumina to remove inhibitors. For flash column chromatography, silica gel with 200–300 mesh was used.

Synthesis of macroinitiator

PBM. Initiator DBI (0.10 g, 0.256 mmol), TBA (9.85 g, 76.88 mmol), CuBr_2 (1.71 mg, 7.68 μmol), and TPMA (8.92 mg, 0.031 mmol) were dissolved in DMF (4 mL) and degassed by purging with nitrogen for 30 min. Polymerization commenced upon the addition of a piece of Cu(0) to the degassed reaction mixture. The solution was stirred at room temperature for 12 h and then precipitated in MeOH/ H_2O mixtures to give the macroinitiator PBM. M_n : 27160; PD: 1.11.

Synthesis of block copolymer

PABE. Macroinitiator PBM (1.5 g, 0.057 mmol), BMA (3.22 g, 22.67 mmol), CuCl_2 (4.60 mg, 0.034 mmol), and PMDETA (11.85 mg, 0.068 mmol) were dissolved in anisole (4 mL). The mixture was degassed by purging with nitrogen for 20 min. After adding degassed stannous octoate (13.86 mg, 0.034 mmol), the mixture was stirred at 70 °C for 20 h. Upon cooling, the catalyst was removed by passing a solution of the polymer in THF over a neutral alumina plug, and then the filtered polymer solution was precipitated in MeOH/ H_2O mixture to give the as-prepared PBBE block copolymer (M_n : 68800; PD: 1.24). Finally, polymer PBBE was dissolved in DCM and 10 mL TFA was slowly added to the mixture. After stirring at room temperature for 24 h, the solution was removed by rotary evaporation to yield amphiphilic block copolymer PABE film. Following the same procedure, PABE-a, PABE-b, PABE-c, and PABE-d block copolymers were prepared by varying the molar feed ratio of PBM/BMA to 1/600, 1/1000, 1/1500, and 1/2000, respectively. To obtain regular test specimens, the above polymer film was further hot pressed in a mold at 120 °C.

Data availability

The authors declare that all the data supporting the findings of this study are provided in the manuscript and its supplementary information files, or available from the corresponding authors on request. Source data are provided with this paper.

References

- Jiang, Y. et al. Topological supramolecular network enabled high-conductivity, stretchable organic bioelectronics. *Science* **375**, 1411–1417 (2022).
- Matsuhisa, N. et al. High-frequency and intrinsically stretchable polymer diodes. *Nature* **600**, 246–252 (2021).
- Yan, Z. et al. Highly stretchable van der Waals thin films for adaptable and breathable electronic membranes. *Science* **375**, 852–859 (2022).
- Xu, S. et al. Illuminating the brain: advances and perspectives in optoelectronics for neural activity monitoring and modulation. *Adv. Mater.* **35**, 2303267 (2023).
- Tan, Y. J. et al. A transparent, self-healing and high- κ dielectric for low-field-emission stretchable optoelectronics. *Nat. Mater.* **19**, 182–188 (2020).
- Larson, C. et al. Highly stretchable electroluminescent skin for optical signaling and tactile sensing. *Science* **351**, 1071–1074 (2016).
- Shi, X. et al. Large-area display textiles integrated with functional systems. *Nature* **591**, 240–245 (2021).
- Jiang, D. H. et al. Facile fabrication of stretchable touch-responsive perovskite light-emitting diodes using robust stretchable composite electrodes. *ACS Appl. Mater. Interfaces* **12**, 14408–14415 (2020).
- Oh, J. H. & Park, J. W. Intrinsically stretchable phosphorescent light-emitting materials for stretchable displays. *ACS Appl. Mater. Interfaces* **15**, 33784–33796 (2023).
- Jeong, M. W. et al. Intrinsically stretchable three primary light-emitting films enabled by elastomer blend for polymer light-emitting diodes. *Sci. Adv.* **9**, eadh1504 (2023).
- Liu, W. et al. High-efficiency stretchable light-emitting polymers from thermally activated delayed fluorescence. *Nat. Mater.* **22**, 737–745 (2023).
- Liang, J., Li, L., Niu, X., Yu, Z. & Pei, Q. Elastomeric polymer light-emitting devices and displays. *Nat. Photon.* **7**, 817–824 (2013).
- Zhang, G., Palmer, G. M., Dewhurst, M. W. & Fraser, C. L. A dual-emissive-materials design concept enables tumour hypoxia imaging. *Nat. Mater.* **8**, 747–751 (2009).
- Bolton, O., Lee, K., Kim, H. J., Lin, K. Y. & Kim, J. Activating efficient phosphorescence from purely organic materials by crystal design. *Nat. Chem.* **3**, 205–210 (2011).

15. Wang, X. et al. Organic phosphors with bright triplet excitons for efficient X-ray-excited luminescence. *Nat. Photon.* **15**, 187–192 (2021).
16. Gao, R., Kodaimati, M. S. & Yan, D. Recent advances in persistent luminescence based on molecular hybrid materials. *Chem. Soc. Rev.* **50**, 5564–5589 (2021).
17. Hamzehpoor, E. et al. Efficient room-temperature phosphorescence of covalent organic frameworks through covalent halogen doping. *Nat. Chem.* **15**, 83–90 (2023).
18. Chen, Z. et al. Synergetic conformational regulations in ground and excited states for realizing stimulus-responsive and wide-tuning room-temperature phosphorescence. *J. Am. Chem. Soc.* **145**, 16748–16759 (2023).
19. Zhao, W. et al. Rational molecular design for achieving persistent and efficient pure organic room-temperature phosphorescence. *Chem* **1**, 592–602 (2016).
20. Garain, S. et al. Anion- π -induced room temperature phosphorescence from emissive charge-transfer states. *J. Am. Chem. Soc.* **144**, 10854–10861 (2022).
21. Ma, X. et al. Supramolecular pins with ultralong efficient phosphorescence. *Adv. Mater.* **33**, 2007476 (2021).
22. Man, Z. et al. Host surface-induced excitation wavelength-dependent organic afterglow. *J. Am. Chem. Soc.* **145**, 13392–13399 (2023).
23. Zhang, Y. et al. Large-area, flexible, transparent, and long-lived polymer-based phosphorescence films. *J. Am. Chem. Soc.* **143**, 13675–13685 (2021).
24. Gan, N. et al. Organic phosphorescent scintillation from copolymers by X-ray irradiation. *Nat. Commun.* **13**, 3995 (2022).
25. Ju, H. et al. Polymerization-induced crystallization of dopant molecules: an efficient strategy for room-temperature phosphorescence of hydrogels. *J. Am. Chem. Soc.* **145**, 3763–3773 (2023).
26. Tian, R., Xu, S. M., Xu, Q. & Lu, C. Large-scale preparation for efficient polymer-based room-temperature phosphorescence via click chemistry. *Sci. Adv.* **6**, eaaz6107 (2020).
27. Ma, X., Xu, C., Wang, J. & Tian, H. Amorphous pure organic polymers for heavy-atom-free efficient room-temperature phosphorescence emission. *Angew. Chem. Int. Ed.* **57**, 10854–10858 (2018).
28. Ren, Y. et al. Clusterization-triggered color-tunable room-temperature phosphorescence from 1,4-dihydropyridine-based polymers. *J. Am. Chem. Soc.* **144**, 1361–1369 (2022).
29. Li, D., Yang, J., Fang, M., Tang, B. Z. & Li, Z. Stimulus-responsive room temperature phosphorescence materials with full-color tunability from pure organic amorphous polymers. *Sci. Adv.* **8**, eabl8392 (2022).
30. Wang, Z. et al. Accessing excitation- and time-responsive afterglows from aqueous processable amorphous polymer films through doping and energy transfer. *Adv. Mater.* **34**, 2202182 (2022).
31. Gmelch, M., Thomas, H., Fries, F. & Reineke, S. Programmable transparent organic luminescent tags. *Sci. Adv.* **5**, eaau7310 (2019).
32. Huang, W., Fu, C., Liang, Z., Zhou, K. & He, Z. Strong circularly-polarized room-temperature phosphorescence from a feasibly separable scaffold of dibenzo[b,d]furan with locked axial chirality. *Angew. Chem. Int. Ed.* **61**, e202202977 (2022).
33. Chen, Y., Kushner, A. M., Williams, G. A. & Guan, Z. Multiphase design of autonomic self-healing thermoplastic elastomers. *Nat. Chem.* **4**, 467–472 (2012).
34. Liu, M., Liu, P., Lu, G., Xu, Z. & Yao, X. Multiphase-assembly of siloxane oligomers with improved mechanical strength and water-enhanced healing. *Angew. Chem. Int. Ed.* **130**, 11412–11416 (2018).
35. Lang, C. et al. Nanostructured block copolymer muscles. *Nat. Nanotechnol.* **17**, 752–758 (2022).
36. Zou, Y., Zhou, X., Ma, J., Yang, X. & Deng, Y. Recent advances in amphiphilic block copolymer templated mesoporous metal-based materials: assembly engineering and applications. *Chem. Soc. Rev.* **49**, 1173–1208 (2020).
37. Bobrin, V. A. et al. Nano- to macro-scale control of 3D printed materials via polymerization induced microphase separation. *Nat. Commun.* **13**, 3577 (2022).
38. Yue, B. et al. In situ regulation of microphase separation-recognized circularly polarized luminescence via photoexcitation-induced molecular aggregation. *ACS Nano* **16**, 16201–16210 (2022).
39. Fernández-Rico, C. et al. Elastic microphase separation produces robust bicontinuous materials. *Nat. Mater.* **23**, 124–130 (2024).
40. Lorandi, F., Fantin, M. & Matyjaszewski, K. Atom transfer radical polymerization: a mechanistic perspective. *J. Am. Chem. Soc.* **144**, 15413–15430 (2022).
41. Chen, X. et al. Versatile room-temperature-phosphorescent materials prepared from N-substituted naphthalimides: emission enhancement and chemical conjugation. *Angew. Chem. Int. Ed.* **55**, 9872–9876 (2016).
42. Li, D. et al. Amorphous metal-free room-temperature phosphorescent small molecules with multicolor photoluminescence via a host-guest and dual-emission strategy. *J. Am. Chem. Soc.* **140**, 1916–1923 (2018).
43. Zheng, Y., Zhang, S., Tok, J. B. H. & Bao, Z. Molecular design of stretchable polymer semiconductors: current progress and future directions. *J. Am. Chem. Soc.* **144**, 4699–4715 (2022).
44. Jiang, D. H. et al. Facile one-pot synthesis of rod-coil bio-block copolymers and uncovering their role in forming the efficient stretchable touch-responsive light emitting diodes. *Chem. Eng. J.* **418**, 129421 (2021).
45. He, C. et al. Super tough and spontaneous water-assisted autonomous self-healing elastomer for underwater wearable electronics. *Adv. Sci.* **8**, 2102275 (2021).
46. Lai, Y. et al. Colorless, transparent, robust, and fast scratch-self-healing elastomers via a phase-locked dynamic bonds design. *Adv. Mater.* **30**, 1802556 (2018).
47. Chen, J. et al. Phase-locked constructing dynamic supramolecular ionic conductive elastomers with superior toughness, autonomous self-healing and recyclability. *Nat. Commun.* **13**, 4868 (2022).

Acknowledgements

This research is supported by the National Natural Science Foundation of China (62288102 (W.H.), 52203242 (L.G.), and 62134007 (W.H.)), National Key R&D Program of China (grant no. 2020YFA0709900 (W.H.)), the Natural Science Foundation of Shaanxi Province (2022JQ-581 (L.G.)), the Natural Science Foundation of Ningbo (2021J054 (L.G.)), the Guangdong Basic and Applied Basic Research Foundation (2021A1515110367 (L.G.)), Zhejiang Provincial Natural Science Foundation of China under Grant No. LQ23B020004 (L.G.). We are grateful to the Analytical & Testing Center of Northwestern Polytechnical University for supporting the test resources.

Author contributions

L.G., Z.A., and W.H. conceived the experiments. N.G., Z.A. and L.G. wrote the manuscript. N. G. and X.Z. conducted the experiments. L.W. helped the characterizations of molecular structures. X.Z. helped to take photos and edit the movies. Z.Q., H.Q., A.L. and H.M. contributed to theoretical calculations. All authors contributed to the data analyses.

Competing interests

The authors declare no competing interests.

Additional information

Supplementary information The online version contains supplementary material available at <https://doi.org/10.1038/s41467-024-47673-y>.

Correspondence and requests for materials should be addressed to Long Gu, Zhongfu An or Wei Huang.

Peer review information *Nature Communications* thanks Chao Lu and the other, anonymous, reviewers for their contribution to the peer review of this work. A peer review file is available.

Reprints and permissions information is available at <http://www.nature.com/reprints>

Publisher's note Springer Nature remains neutral with regard to jurisdictional claims in published maps and institutional affiliations.

Open Access This article is licensed under a Creative Commons Attribution 4.0 International License, which permits use, sharing, adaptation, distribution and reproduction in any medium or format, as long as you give appropriate credit to the original author(s) and the source, provide a link to the Creative Commons licence, and indicate if changes were made. The images or other third party material in this article are included in the article's Creative Commons licence, unless indicated otherwise in a credit line to the material. If material is not included in the article's Creative Commons licence and your intended use is not permitted by statutory regulation or exceeds the permitted use, you will need to obtain permission directly from the copyright holder. To view a copy of this licence, visit <http://creativecommons.org/licenses/by/4.0/>.

© The Author(s) 2024